ELSEVIER

Catalysis Today 39 (1998) 329–341

CATALYSIS TODAY

Study on a cobalt silica catalyst during reduction and Fischer–Tropsch reaction: In situ EXAFS compared to XPS and XRD

B. Ernst[a], A. Bensaddik[a], L. Hilaire[a], P. Chaumette[b], A. Kiennemann[a,*]

[a]LERCSI-ECPM, URA CNRS 1498, 1, rue Blaise Pascal, 67008 Strasbourg Cedex, France
[b]Institut Francais du Petrole, 1-4, Avenue de Bois Préau BP 311, 92506 Rueil Malmaison Cedex, France

Abstract

The reduction of a 25 wt% Co/SiO_2 catalyst for the hydrocarbon synthesis has been followed by several techniques: XRD, TPR, XPS and in situ EXAFS. Before reduction the cobalt is present as a Co_3O_4 spinel phase. A two-step reduction of Co_3O_4 to CoO and then to Co° is observed by EXAFS. This is consistent with XPS (surface) and TPR or XRD (bulk) studies. During CO/H_2 reaction, cobalt is always in the metallic state (EXAFS). The coordination number of cobalt has been determined at each reduction step and during CO hydrogenation reaction. © 1998 Elsevier Science B.V.

Keywords: In situ EXAFS; Cobalt; Fischer–Tropsch; Reducibility

1. Introduction

Cobalt is one of the most studied metals in Fischer–Tropsch synthesis. This metal is active and has a good selectivity to alcohol or linear hydrocarbons, to short (C_2–C_4) or very long (C_{20}–C_{60}) chains, to paraffins or olefins, depending on the reaction conditions, on the metal promoter (Cu, Ru, Mn, etc.), on the oxide promoter (rare earth oxides, TiO_2, etc.) or on the nature of the support (SiO_2, Al_2O_3, etc.) [1]. Moreover cobalt leads to the formation of water and not of CO_2 (loss of a carbon atom) and its carburization is low compared to that of iron based catalysts.

It is generally admitted, but rarely demonstrated in reaction conditions, that the active phase is a cobalt metal. The active phase is dispersed on high specific surface area support (Al_2O_3, SiO_2), with which the formation of well-defined structures like $CoAl_2O_4$ or Co_2SiO_4 spinels must be avoided. On these cobalt catalysts, there is a controversy concerning the structure sensitivity in the Fischer–Tropsch reaction when the metal is deposited on different supports. It has been shown that the dispersion of the cobalt active phase has an influence on the chain growth [2] and allows to explain the hydrocarbon distributions which do not follow the conventional Anderson–Schulz–Flory model (ASF) [3]. It has also been observed that well-dispersed cobalt on silica favours the formation of short chain hydrocarbons and oxygenated compounds [4]. However, Iglesia et al. [5–7] have shown that at high CO conversion, the reaction becomes structure insensitive with very slight changes in the methane selectivity and the C_{5+} hydrocarbon formation with dispersions ranging from 0.45% to 9.5%. In fact, the metal particle size and thus the dispersion is governed by numerous parameters like preparation method, nature of the support, catalyst reduction

---

*Corresponding author.

0920-5861/98/$32.00 © 1998 Elsevier Science B.V. All rights reserved.
PII S0920-5861(97)00124-7

procedure, reaction conditions, etc. Therefore, it is important to well characterize the reduced state of the catalysts used in Fischer–Tropsch synthesis to obtain high molecular weight hydrocarbons. The aim of the present work will be to describe the reduction state of one of our catalysts (25 wt% Co/SiO_2) before, during and after the reactivity tests. The reduction state has been characterized by various techniques: X-ray diffraction (XRD), transmission electron microscopy (TEM), X-ray photoelectron spectroscopy (XPS), temperature programmed reduction (TPR) and more essentially by in situ EXAFS (extended X-ray absorption fine structure) during the reduction and the reactivity tests in syngas atmosphere.

2. Experimental

2.1. Catalyst preparation

The 25 wt% Co/SiO_2 catalyst was prepared according to the following procedure: 15 g of cobalt nitrate ($Co(NO_3)_2$, $6H_2O$) and 25.2 g of tetraethoxysilane (98% purity) were dissolved in 300 and 200 ml of ethanol, respectively. The solutions were heated to 343 K and mixed to give solution A. A solution of 7.1 g oxalic acid (10 wt% in excess) in 100 ml ethanol was added to solution A to precipitate the cobalt nitrate (pH<1). The alcohol was then slowly evaporated and the tetraethoxysilane was hydrolysed by the crystallization water of the precursors: cobalt nitrate and oxalic acid. After drying (383 K, 12 h) and calcination (823 K, 5 h), the catalyst noted as 25 wt% Co/SiO_2 has a BET surface area of 293 m^2 $gcat^{-1}$. Its weight composition is: Co=25.3 wt%; Si=28.4 wt%; O=46.1 wt%.

2.2. Experimental techniques

2.2.1. In situ extended X-ray absorption fine structure (EXAFS)

The EXAFS measurements were performed at the LURE synchrotron centre (ORSAY – France) using the electromagnetic radiation issued from the DCI storage ring with an energy of 1.85 GeV. The EXAFS spectra were recorded at the cobalt K-edge (7708.9 eV). The white polychromatic beam was monochromatized using a double Bragg reflection on Si(1 1 1) single crystals. The X-ray absorption measurements were performed in the transmission mode. The detection system is composed of two ionization chambers for the measurement of the intensity of the beam before and after transmission through the sample. The thickness of the 25 wt% Co/SiO_2 catalyst pellets was between 100 and 200 μm in order to allow a better gas circulation. The reactor used in the in situ measurement was similar to the one designed by Lytle et al. [8,9] and is given in Fig. 1. It was equipped with:

- a heating device for working in a wide temperature range (290 K<T<900 K),
- a gas admission device (H_2, CO, N_2, etc.),
- a controlled gas flow-rates (5 ml min^{-1}),
- two 50 μm thick kapton windows.

The EXAFS formalism and analytical procedure used is a standard one [10]. Fourier transforms of the k^3 weighted EXAFS functions were obtained using a 12 Å^{-1} Hanning type window. By inverse Fourier transform (1.61–3.21 Å filter), the filtered EXAFS modules corresponding to the analysis of the desired shell were obtained. The structural parameters (number of nearest neighbours, interatomic distances, etc.) were determined using the experimental phase shifts and backscattering amplitudes extracted from the appropriate experimental references. In this work, cobalt foil, CoO and Co_3O_4 were used as references for the Co–Co and Co–O absorber–scatterer pairs. As usual, the radial distribution functions (RDFs) (Fourier transforms), which are presented in this article, refer to the distance values uncorrected for phase shift, whereas real interatomic distances, i.e., values corrected for phase shift, are given in the text and Tables 3 and 4. All the refinements have been performed in the energy (E) and distance (R) spaces.

2.2.2. X-ray photoelectron spectroscopy (XPS)

The spectrometer was a Vacuum Generator ESCA3 possessing two chambers. It is composed of a sample introduction and preparation chamber including a gas (H_2) admission device at atmospheric pressure and an analysis chamber at a vacuum of 10^{-10} Torr. The sample was pelleted (∼50 mg) and set on a sample-holder with a heating device (293 K<T<873 K). The decomposition of the various peaks was described elsewhere [11] and includes the following parameters:

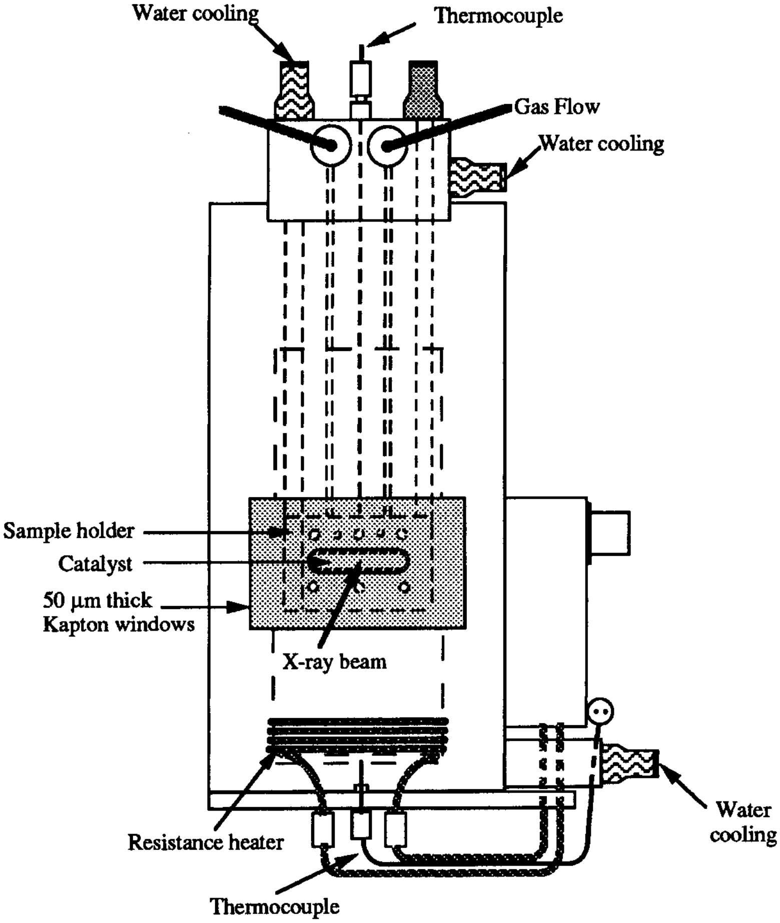

Fig. 1. Diagram of the in situ EXAFS reaction system (transmission mode).

energy of the peaks (E), asymmetry factor (α), full width at half maximum (2γ) and relative intensities (I). In the present work the decompositions were made on both $Co2p_{3/2}$ and $Co2p_{1/2}$ peaks. The binding energies were measured by taking the C1s peak of the contamination carbon at 284.8 eV as a reference.

2.2.3. X-ray diffraction (XRD)

The X-ray monochromatic beam was produced by a Cu anticathode (λ=1.5418 Å). The apparatus was a powder diffractometer Siemens D5000 device. The XRD patterns were recorded for 2θ between 10° and 90° with a 0.005° 2θ spacing and 3 s exposure time. The identification of the phases was made with the help of the JCPDS files (Joint Committee on Powder Diffraction Standards).

2.2.4. Temperature programmed reduction (TPR)

The TPR experiments were done by passing pure hydrogen at a flow rate of 12 ml min^{-1} (temperature increasing rate: 1 K min^{-1}) or by passing a gas mixture of 5% H_2 in He at a total flow rate of 50 ml min^{-1} (temperature increasing rate: 15 K min^{-1}) over the calcined sample. Sample weight of 0.2 g was used. The detection system was a catharometer which allows to monitor the formation of water or, after a removal trap, the hydrogen consumption.

2.2.5. Transmission electron microscopy (TEM)

The apparatus was a TOPCON EM-002B type device. Its resolution is 1.8 Å. The acceleration potential is 200 kV. The analysis of the chemical elements is done by EDS with a KEVEC analyser (diameter of the selected area=14 nm). The powdered sample was suspended in ethanol. One drop of the suspension was deposited on a copper grid covered by a fine carbon membrane evaporated under vacuum. Selected area diffraction (diameter=200 Å) was used for microdiffraction.

3. Results and discussion

3.1. Characterization of the starting catalyst

The transmission electron micrograph (TEM) (Fig. 2) shows that the silicon oxide is in the form of rafts. Cobalt particles of inhomogeneous size between 80 and 350 Å can also be seen.

After calcination, two types of structures could be present: Co_3O_4 (a=8.084 Å) and Co_2SiO_4 (a=8.140 Å). These two structures have almost similar interreticular distances and only the respective intensity of the secondary lines will allow an effective discrimination. The XRD pattern obtained for the 25 wt% Co/SiO_2 catalyst is given on Fig. 3, as well as the comparative table of the Co_3O_4, Co_2SiO_4 and 25 wt% Co/SiO_2 lines with their respective intensities (Table 1). On the experimental XRD pattern of the 25 wt% Co/SiO_2 catalyst (Fig. 3), the Co_3O_4 reference compound (vertical lines), issued from JCPDS file 42-1467, has been added.

Table 1
XRD lines comparison of Co_3O_4 (reference), Co_2SiO_4 (reference) and for the 25 wt% Co/SiO_2 catalyst

Reference Co_2SiO_4	Reference Co_3O_4	25 wt% Co/SiO_2
2.454[a] (100)	2.437 (100)	2.430 (100)
4.700 (47)	1.429 (38)	1.429 (38)
2.035 (44)	2.838 (33)	2.845 (25)
1.439 (34)	1.556 (32)	1.555 (36)
1.566 (21)	2.021 (20)	2.016 (17)
2.350 (13)	4.667 (16)	4.660 (14)

Values given in parenthesis represent relative intensity.
[a] Interreticular distance (Å).

In Table 1, the comparison of the intensity of the secondary lines leads to the conclusion that the cobalt from the 25 wt% Co/SiO_2 catalyst is essentially present as Co_3O_4. However, the presence of amorphous or microcrystalline Co_2SiO_4 phase, not detected by XRD, cannot be totally excluded. The formation of cobalt silicate is therefore limited as compared to the Co/Al_2O_3 catalyst for which the $CoAl_2O_4$ spinel can be readily formed [12]. This is important since the cobalt, once involved in such a structure, is very difficult to reduce and therefore remains inactive in Fischer–Tropsch synthesis. For our catalyst, the particle size of the cobalt oxide could be evaluated by XRD (line broadening Debye–Scherrer method). The mean size of Co_3O_4 is about 300 Å. For the catalyst reduced by H_2, the contact with well-controlled

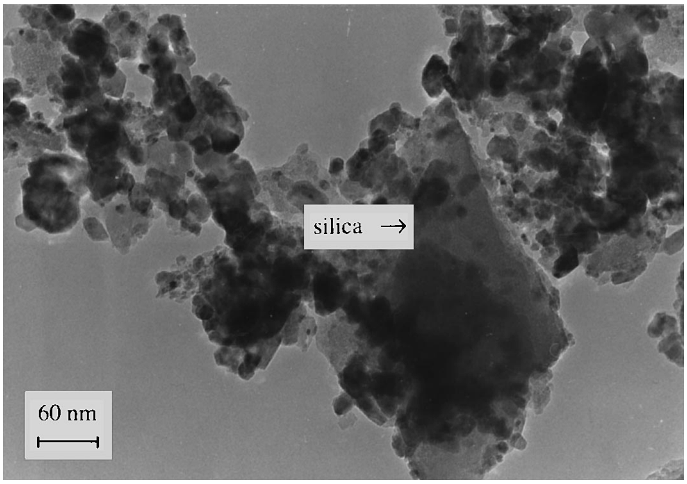

Fig. 2. TEM image of the 25 wt% Co/SiO_2 catalyst.

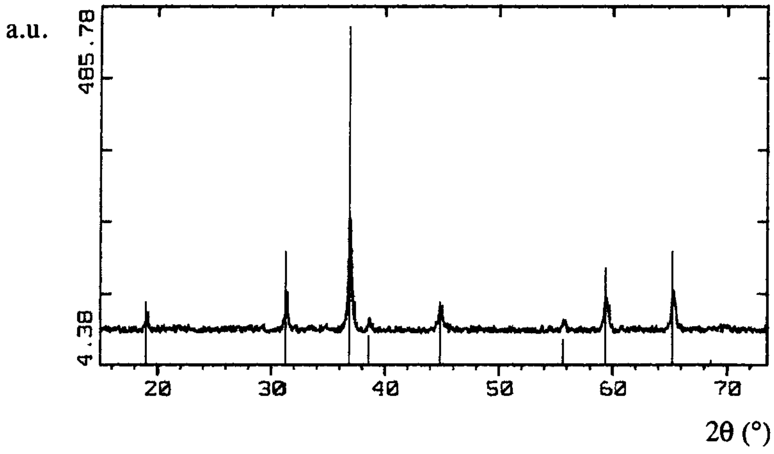

Fig. 3. XRD pattern of the 25 wt% Co/SiO_2 catalyst before reduction. Vertical lines correspond to the Co_3O_4 reference lines issued from the JCPDS file 42-1467.

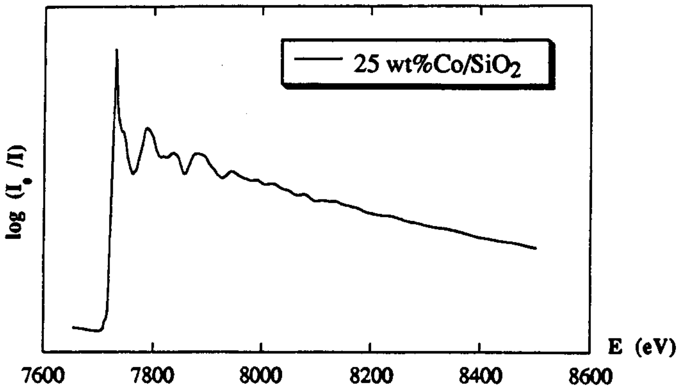

Fig. 4. X-ray absorption spectrum (cobalt K-edge) of the untreated 25 wt% Co/SiO_2 catalyst.

amounts of oxygen at 673 K until total oxidation of Co° to Co_3O_4 allows to measure the oxide particle size by XRD [13] (about 240 Å). Thus, after reduction–reoxidation procedure, the particle size of the oxide Co_3O_4 decreases compared to the initial particle size. This indicates that there is no coalescence of the particles during the reduction.

The study of the EXAFS spectra for the catalyst before treatment recorded at the cobalt K-edge can also be used to estimate the oxidation state of the cobalt. The absorption spectrum of the catalyst sample, introduced into the cell before hydrogen treatment, is given in Fig. 4.

The comparison of the RDF (Fourier transform module) of the calcined catalyst with the two cobalt oxide (Co_3O_4 and CoO) references shows that it is similar to the RDF of the Co_3O_4 reference (Fig. 5).

By XPS, the decomposition of the $Co2p_{3/2}$ and $Co2p_{1/2}$ peak allows, before reduction, to determine the respective amounts of Co^{3+} (octahedral) (peak at 779.7 eV=61.2%); Co^{2+} (tetrahedral) (peak at 781.5 eV=30.6%) and the satellite (peak at 787.6 eV=8.2%) confirming thus the presence of Co_3O_4 before reduction. The absence of Co_2SiO_4 is confirmed on the surface.

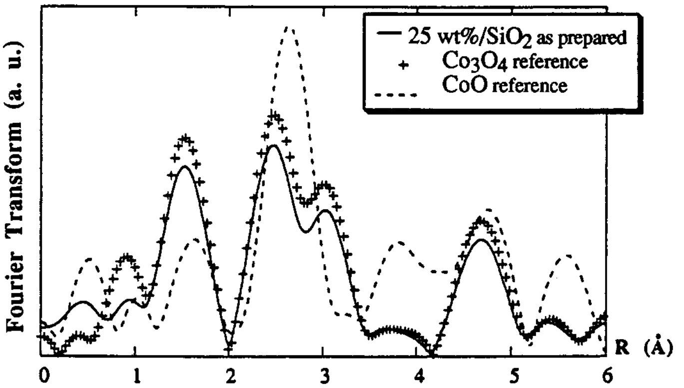

Fig. 5. Comparison of the EXAFS RDFs of the untreated 25 wt% Co/SiO_2 catalyst and the model compounds (Co_3O_4 and CoO).

3.2. *Study of the reduction of the 25 wt%* Co/SiO_2 *catalyst*

The temperature programmed reduction gives a first approach of the temperature range for the reduction of Co_3O_4 to metal Co. A particular attention has been given to the optimization of the parameters: temperature rate, reactant gas (H_2) concentration in the carrier gas (Ar, He, N_2), mass of catalyst, total gas flow to be in agreement with the criteria defined in the literature [14,15]. The value of the criterion $P=\beta S_0/FC_0$, where β is the temperature increasing rate (K s^{-1}), F the total flow rate (cm^3 s^{-1}), C_0 the initial hydrogen concentration (mol cm^{-3}) and S_0 is the amount of reducible species present in the sample (mole), must be as low as possible and in all cases lower than 20 K. In the present study it was 6.2 K. Under these conditions, the reduction profile (TPR) of the 25 wt% Co/SiO_2 catalyst between 293 and 1073 K is represented in Fig. 6. It is compared to that of the Co_2SiO_4 spinel.

In CO/H_2 reactivity measurements, the catalyst is reduced at a maximum temperature of 753 K, therefore the TPR reduction profile was established up to 773 K at a low temperature increasing rate (1 K min^{-1} instead of 15 K min^{-1}) (P=1.4 K) in conditions those are near that used in the reduction for the reactivity studies under pressure. Both profiles show two peaks which shift to lower temperatures for the TPR with the lowest temperature increasing rate (533 K instead of 663 K for the first sharp peak), (653–673 K compared

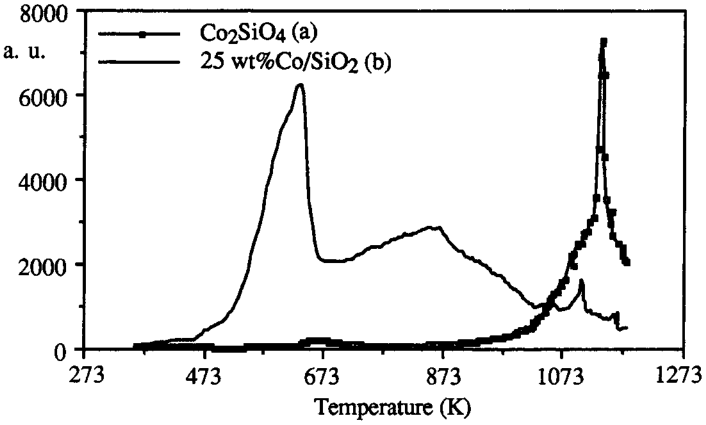

Fig. 6. Temperature programmed reduction profile of Co_2SiO_4 (a) and the 25 wt% Co/SiO_2 catalyst (b).

to 823–833 K for the second broader peak). A sharp but very weak peak is observed at temperatures higher than 1073 K (high temperature reduction). This last peak has been attributed to cobalt silicate (see Fig. 6). It must be noted that no cobalt silicate was detected in XRD, XPS or EXAFS experiments. It must be admitted that cobalt silicate could preexist as dispersed microcrystals or that it is formed at high temperature during TPR. According to the literature studies the reduction of Co_3O_4 is relatively complex. Depending on the experimental conditions [16], it can be shown that two distinct reduction peaks are observed for bulk Co_3O_4. The areas ratio of the two peaks is 3/1 in agreement with the following scheme:

$$Co_3O_4 + H_2 \rightarrow 3CoO + H_2O \qquad (1)$$

$$3CoO + 3H_2 \rightarrow 3Co^\circ + 3H_2O. \qquad (2)$$

For the supported catalyst, it is more difficult to distinguish between the two reduction peaks since the cobalt dispersion, the homogeneity or heterogeneity in particle size, the texture of the support can modify the TPR profile [17]. For our catalyst, it is not possible to attribute the two reduction peaks to the two steps $Co_3O_4 \rightarrow CoO \rightarrow Co^\circ$, because the separation between the two maxima is too high (more than 100 K). It can rather be suggested that they are the consequence of the reduction of cobalt oxides which have different interaction strengths with the support. This interaction would be dependent on the size of the metal oxide particles. The particles of higher size which would interact less with the support would be reduced first. The size heterogeneity is shown by the TEM image (Fig. 2). Another possible explanation could be the difficulty to eliminate the reduction water for the low size particle deposited in the low diameter pores [18]. In our case, this last hypothesis could hold because of the observed pore volume distribution. Indeed 90% of the 293 m^2 g cat^{-1} surface area as measured by BET can be attributed to micropores and the remaining 10% to mesopores.

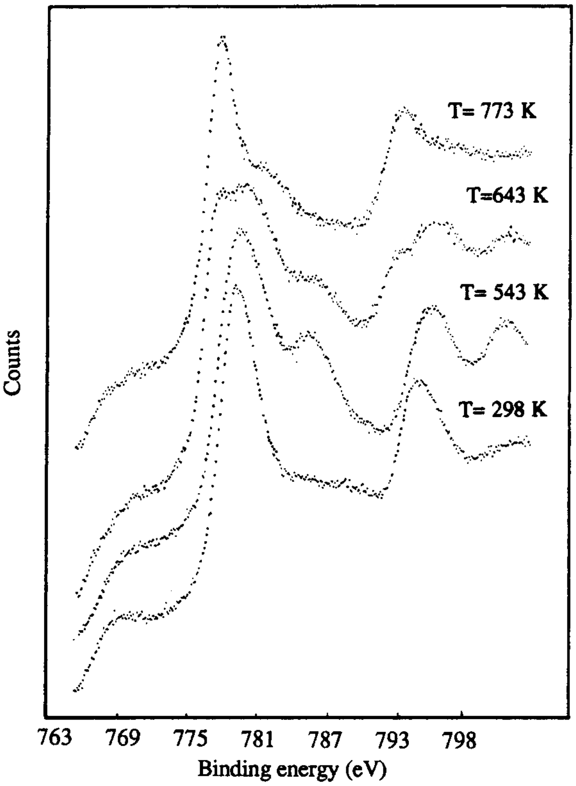

Fig. 7. Cobalt 2p XP spectra of the 25 wt% Co/SiO_2 catalyst unreduced, reduced at 543, 643 and 773 K.

On the surface, however, the $Co_3O_4 \rightarrow CoO \rightarrow Co^\circ$ pathway can be evidenced by XPS. The change in the reduction state of the surface as followed by XPS for the 25 wt% Co/SiO_2 between 293 and 773 K is represented in Fig. 7. The binding energies, as well as the percentage of each species, are summarized in Table 2, assuming that from 543 K upwards the Co_3O_4 structure has collapsed and the whole peak

Table 2
XPS study of the reduction of the 25 wt% Co/SiO_2 catalyst

Reduction temperature (K)	Co^{3+} (octahedral)	Co^{2+} (tetrahedral)	Co^{2+} (octahedral)	Co (metal)
T=298 K	69% (779.7 eV)	31% (781.5 eV)		—
T=543 K	52% (779.8 eV)	—	48% (781.8 eV)	—
T=643 K	37% (779.9 eV)	—	21% (781.9 eV)	42% (777.9 eV)
T=773 K	—	—	18% (781.7 eV)	82% (777.7 eV)

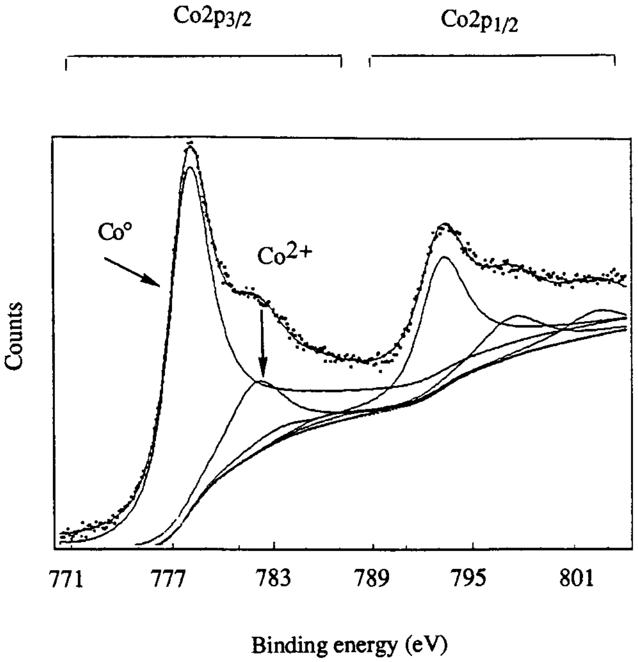

Fig. 8. Decomposed cobalt 2p XP spectrum of the 25 wt% Co/SiO_2 catalyst reduced at 773 K.

in 781.7 eV region is due to CoO. At the reduction temperature of 543 K, the cobalt presents two contributions: Co^{3+} (octahedral), attesting the presence of Co_3O_4, and Co^{2+} (octahedral) for CoO. The contribution of the metallic cobalt is absent. At 643 K, the three phases Co_3O_4, CoO and metallic cobalt are represented and the reduction rate is evaluated at 41.5%. Thus, the two reduction steps (CoO_3O_4→CoO and CoO→Co°) are simultaneous. At 773 K, the only phases present are the metallic cobalt (82%) and CoO (18%). The decomposition of the Co2p XP spectrum for the 25 wt% Co/SiO_2 catalyst reduced at 773 K is given in Fig. 8. It includes also the contribution of the shake-up satellite of Co^{2+}.

In order to have a better insight into the reduction of the bulk, in situ EXAFS measurements were performed between 293 and 673 K. For each reduction step, the absorption spectra at the K-edge of cobalt were recorded after cooling down to room temperature in order to optimize the signal/noise ratio. The sample remained under the reactant gas flow. A metal cobalt foil, and Co_3O_4 and CoO powders were used as references. The first spectrum was recorded after reduction at 473 K (0.5 h). At that temperature, the cobalt was still present as Co_3O_4 and its reduction had not started. However, the comparison between the starting catalyst and the catalyst reduced at 553 K shows a change in the environment of cobalt (Fig. 9).

As indicated in Fig. 10, we notice the presence of CoO and Co°; the phase Co_3O_4 is only present as trace amounts. Table 3 gives the structural parameters at the K-edge of cobalt for the catalyst reduced at 553 K.

The Co–O bonds (Table 3) detected are essentially related to the reference CoO and not to Co_3O_4. It can be observed that the reduction of cobalt has indeed started since the number of Co–Co bonds

Table 3
EXAFS parameters (cobalt K-edge) of the 25 wt% Co/SiO_2 catalyst reduced at 553 K (the attribution of the phases has been done using the reference spectra of pure compounds)

Number and nature of the neighbours	Distances (Å)	Debye–Waller factor	Phase
$N_{Co–O}=0.7$	$R_{Co–O}=1.91$	$\Delta\sigma=0.03$	Co_3O_4
$N_{Co–O}=3.0$	$R_{Co–O}=2.10$	$\Delta\sigma=0.00$	CoO
$N_{Co–Co}=3.4$	$R_{Co–Co}=3.02$	$\Delta\sigma=0.00$	CoO
$N_{Co–Co}=4.7$	$R_{Co–Co}=2.51$	$\Delta\sigma=0.00$	Co metal

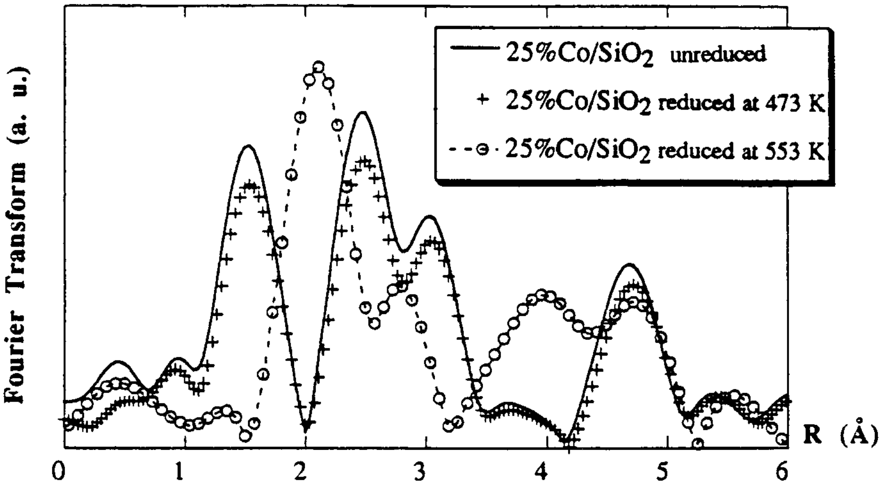

Fig. 9. Comparison between the EXAFS RDFs (cobalt K-edge) of the 25 wt% Co/SiO_2 unreduced (—), reduced at 473 K (++++) and reduced at 553 K (oooo).

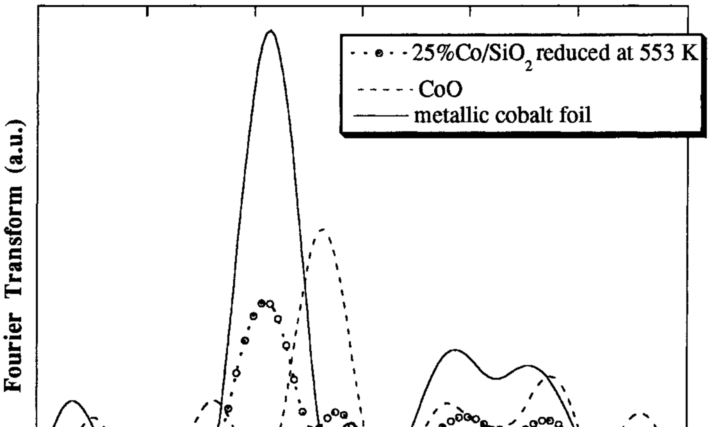

Fig. 10. Comparison between the EXAFS RDFs (cobalt K-edge) of the 25 wt% Co/SiO_2 reduced at 553 K and the model compounds (CoO and Co foil).

(N_{Co-Co}=4.7) becomes nearer to that of the metal reference. The simultaneous presence of CoO and Co° has also been observed by XPS previously, but at a higher reduction temperature (773 K) showing that the different reduction mode (static for XPS and dynamic for EXAFS measurements) influences the reduction rate of the cobalt.

At 673 K, the EXAFS RDF is very similar to that of the metallic cobalt reference (Fig. 11). Fig. 12 gives an example of the quality of agreement between the experimental and calculated spectra. Moreover the numerical simulation gives a coordination sphere containing only cobalt atoms at a Co–Co distance of 2.51 Å. The calculated number of neighbours is 7.8

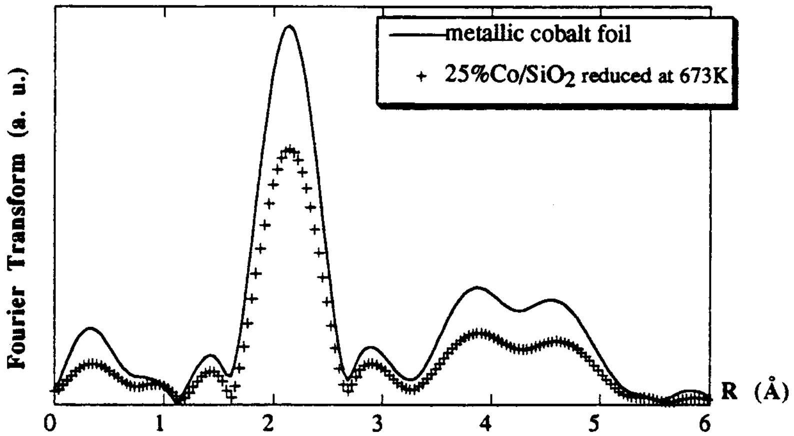

Fig. 11. Comparison between the EXAFS RDFs (cobalt K-edge) of the 25 wt% Co/SiO_2 catalyst reduced at 673 K and metallic cobalt.

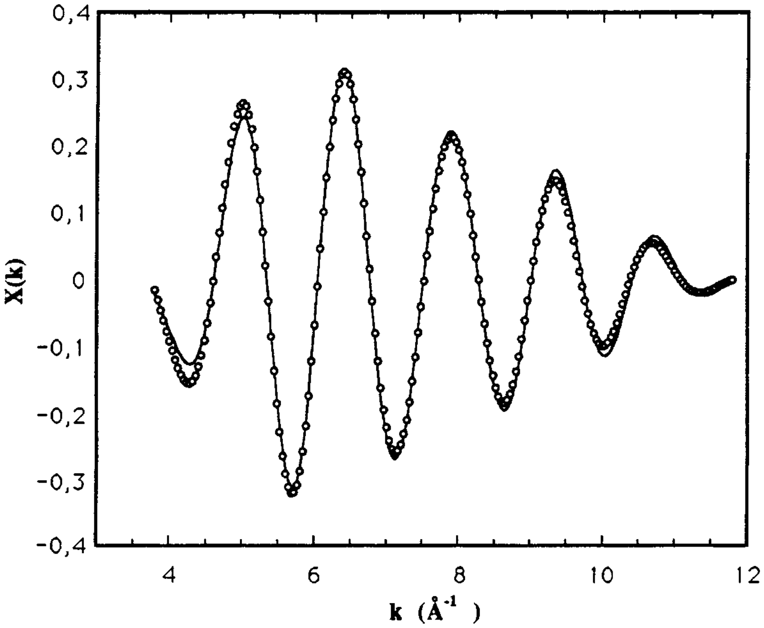

Fig. 12. Comparison of the imaginary and absolute k^3 weighted Fourier transforms (cobalt K-edge) for the experimental spectrum (oooo) and the theorical spectrum (solid line) of the 25 wt% Co/SiO_2 catalyst reduced at 673 K in E space.

(Table 4, line A) which is relatively far from 12 obtained for the metal foil and thus confirms the important proportion of small particles [19].

As a summary, the studies on the 25 wt% Co/SiO_2 catalyst allow to evaluate its reduction at different temperatures by various bulk and surface techniques. The Co_3O_4 phase could be characterized before reduction and the absence of cobalt silicate could be evidenced. The reduction of the Co_3O_4 spinel to CoO then to Co° could be shown by XPS and in situ EXAFS. At 673 K, almost all the cobalt is reduced to the metal state and the number of Co–Co coordination is low (7.8) compared to the cobalt foil (N=12).

Table 4
EXAFS parameters (cobalt K-edge) of the 25 wt% Co/SiO_2 catalyst

	Number of the neighbours	Distances (Å)	Debye–Waller factor
(A)	$N_{Co–Co}=7.8$	$R_{Co–Co}=2.51$	$\Delta\sigma=0.000$
(B)	$N_{Co–Co}=5.1$	$R_{Co–Co}=2.51$	$\Delta\sigma=0.010$

(A) after reduction at 673 K ($T=293$ K, the temperature at which the spectra have been taken; (B) after two hours CO/H_2 reaction at 493 K ($T=493$ K, the temperature at which the spectra have been taken).

3.3. Reduction state of cobalt during and after the $CO + H_2$ *reaction*

The $CO+H_2$ reaction has been performed at atmospheric pressure at 493 K directly in the EXAFS cell. This temperature is often used in hydrocarbon synthesis on cobalt based catalysts [20]. The catalyst is active in these conditions since the formation of C_1 and C_2 hydrocarbons are observed by gas chromatography during the reaction. However, these are not the optimal reaction conditions since, in the conventional reaction, the 25 wt% Co/SiO_2 catalyst works under pressure (2 MPa) for the formation of heavy hydrocarbons [20]. The catalysts after reactivity test under pressure or in the EXAFS cell have both been characterized by electron diffraction. This ex situ characterization shows the characteristic lines (first and second line intensity) of hexagonal (1.91 Å, 2.05 Å) and cubic Co (2.05 Å, 1.77 Å) but some uncertainty exists between Co° and CoO (first line of CoO at 2.13 Å). The in situ EXAFS characterizations during the reactivity test are more conclusive. The Fourier transform of the EXAFS spectrum (taken at 293 K) of the catalyst reduced at 673 K, compared to that obtained during the reaction (2 h $CO–H_2$ reaction at 493 K) (taken at 493 K) are given in Fig. 13. From these spectra it can be concluded that cobalt remains at the zero oxidation state. This is in agreement with the work of Huffman et al. [19] on cobalt catalysts with a

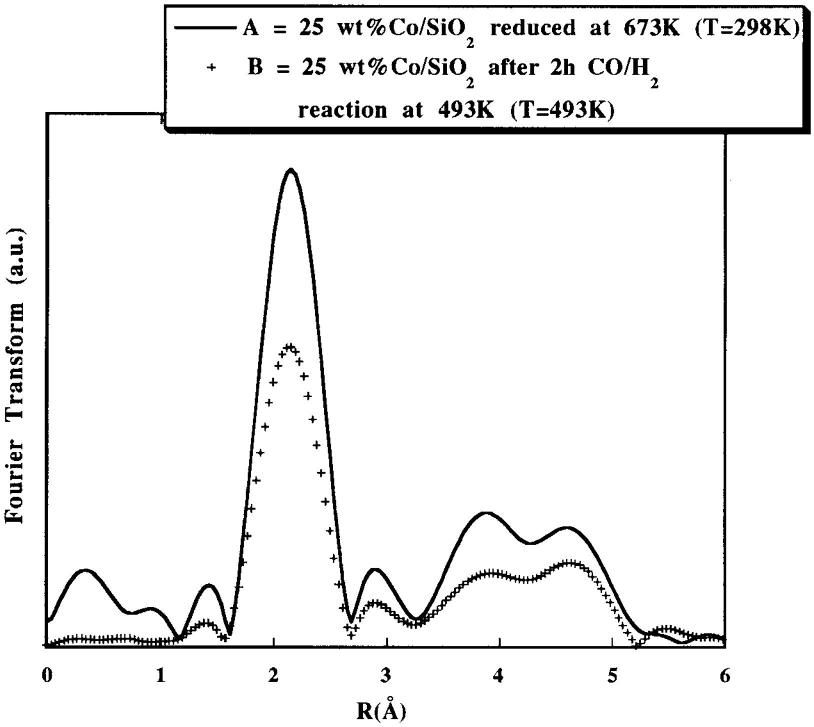

Fig. 13. EXAFS RDFs (cobalt K-edge) of the 25 wt% Co/SiO_2 catalyst: (A) after reduction at 673 K, ($T=293$ K, the temperature at which the spectra have been taken); (B) after two hours CO/H_2 reaction at 493 K ($T=493$ K, the temperature at which the spectra have been taken).

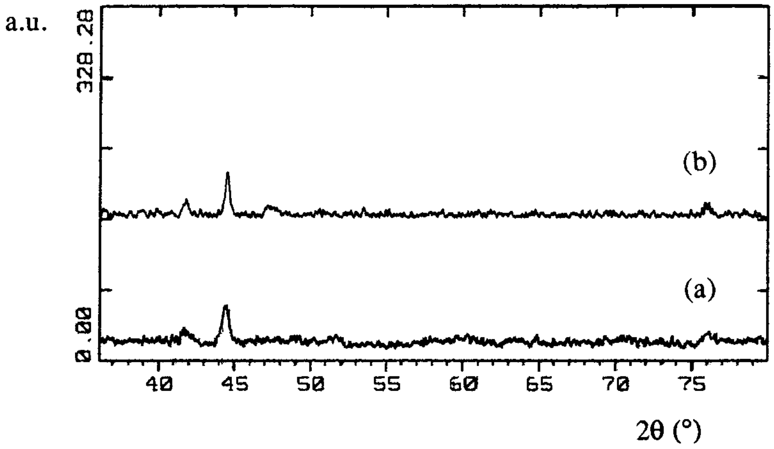

Fig. 14. XRD patterns of the 25 wt% Co/SiO_2 catalyst after reduction at 673 K (a) and after CO/H_2 reaction under pressure (2 MPa, T=220°C, $H_2/CO=2$, V.V.H.=2000 h^{-1}).

lower cobalt content (4.4 wt% Co/SiO_2) (XANES) as well as on a 9 wt% Co/Al_2O_3 catalyst (EXAFS). The interatomic distances (R), the coordination number (N) and the difference ($\Delta\sigma$) of the Debye–Waller coefficient between the sample and the reference are given in Table 4.

Table 4 and Fig. 13 show that the reduction state of the cobalt present on the catalyst is similar to that on the foil used as a reference in terms of Co–Co distance (2.51 Å). This is in agreement with our XRD patterns (Fig. 14) showing that after CO/H_2 reaction under pressure (2 MPa), as after reduction at 673 K, the only phase present is the cubic cobalt structure (main line intensity at 2.05 Å). Thus, even in presence of water, formed during the reaction, the cobalt remains in the metallic state. But the number of neighbours, calculated by EXAFS, is different: 12 for the foil, 7.8 for the reduced catalyst and 5.1 only for the working catalyst under $CO+H_2$. This point suggests that small metal particles are formed during the reduction and are split during the reaction. Huffman et al. [19] have found a coordination number of 6.3 and 5.4 respectively, after reduction and $CO–H_2$ reaction. Assuming the model of Greegor and Lytle [21], the average cobalt particle size has been estimated at 10–20 Å. It seems that this value is smaller than the actual cobalt particle size for the impregnated 9.0 wt% Co/Al_2O_3 catalyst [19] and for our catalyst. The problem about the agreement of the result and the ΔN uncertainty on the values of N arises. ΔN is in general less than 20% [22]. However as indicated in [19], ΔN can be significantly higher than 20% if the calculation involves more than one shell and is extended to the coordination shells beyond the nearest shells. It must also be remembered that the particle size determined through the EXAFS mean coordination number is lower than it really is [23,24].

4. Conclusion

The reduction of a 25 wt% Co/SiO_2 which is used in the production of heavy hydrocarbons in $CO–H_2$ synthesis has been studied by various methods (TPR, XRD, XPS) and by in situ EXAFS during reaction. It could be shown by this latter technique that cobalt is completely reduced to the metal state by H_2 at 673 K and remains in the metal state all along the CO/H_2 reaction at 493 K. In the limit of sensitivity of the methods no other forms of cobalt could be detected (CoO, Co_3O_4, carbide) on the working catalysts.

Acknowledgements

This work was, in part, supported by grants from the European Community Program COST D5. The authors gratefully acknowledge J.L. Schmitt (LERCSI), D. Bazin (LURE) and F. Villain (LURE) for their expert assistance in EXAFS measurements.

References

[1] L. Guczi (Ed.), Stud. Surf. Sci. Catal. 64 (1991).
[2] R.C. Reuel, C.H. Bartholomew, J. Catal. 85 (1984) 78.
[3] Y. Yang, S. Pen, B. Zhang, Catal. Lett. 16 (1992) 351.
[4] T. Matsuzaki, K. Takeuchi, H. Arakawa, T. Hanaoka, Y. Sugi, Shokubai, 32 (1990) 71.
[5] E. Iglesia, S.L. Soled, R.A. Fiato, J. Catal. 137 (1992) 212.
[6] E. Iglesia, Adv. Catal. 39 (1993) 221.
[7] S. Soled, E. Iglesia, R.A. Fiato, Catal. Lett. 7 (1990) 271.
[8] F.W. Lytle, P.S.P. Wei, R.B. Greegor, G.H. Via, J.H. Sinfelt, J. Chem. Phys. 70 (1979) 4849.
[9] F.W. Lytle, R.B. Greegor, E.C. Marques, D.R. Sandstrom, G.H. Via, J.H. Sinfelt, J. Catal. 95 (1985) 546.
[10] B.K. Teo, in: EXAFS: Basic Principles and Data Analysis, Springer, Berlin, 1986.
[11] M. Romeo, K. Bak, J. El Fallah, F. Le Normand, L. Hilaire, Surf. Interface Anal. 20 (1993) 508.
[12] R.L. Chin, D.M. Hercules, J. Phys. Chem. 86 (1982) 360.
[13] S.H. Moon, K.E. Yoon, Appl. Catal. 16 (1985) 289.
[14] D.A.M. Monti, A. Baiker, J. Catal. 83 (1983) 323.
[15] P. Malet, A. Caballero, J. Chem. Soc. Farad. Trans. I 84 (1988) 2369.
[16] B. Sexton, A.E. Hughes, T.W. Turney, J. Catal. 97 (1986) 390.
[17] D.G. Castner, P.R. Watson, I.Y. Chan, J. Phys. Chem. 94 (1990) 819.
[18] N.W. Hurst, S.J. Gentry, A. Jones, B.D. Mc Nicol, Cat. Rev. Sci. Eng. 24 (1982) 233.
[19] G.P. Huffman, N. Shah, J. Zhao, F.E. Huggins, T.E. Hoost, S. Halvorsen, J.G. Goodwin, J. Catal. 151 (1995) 17.
[20] M.E. Dry, Catal. Today 6 (1990) 183.
[21] R.B. Greegor, F.W. Lytle, J. Catal. 63 (1980) 476.
[22] P. Eisenberg, B. Lengeler, Phys. Rev. B 22 (1980) 3351.
[23] J. Zhao, P.A. Montano, Phys. Rev. B 40 (1989) 3401.
[24] A.T. Ashcroft, A.K. Cheetham, P.J.F. Harris, R.H. Jones, S. Natarajan, G. Sankar, N.J. Stedman, J.M. Thomas, Catal. Lett. 24 (1994) 47.